Brain Tumor Segmentation and Area Calculation using Convolutional Neural Networks

Chandrasekara E.S.K

SC/2018/10559

Submitted in partial fulfillment of the requirements for the award of the degree of
PHY 2b22

BSc (General) Physical Science

Faculty of Science

University of Ruhuna

2021

Certificate

I hereby certify that the work which is being presented in the B.Sc. General Degree (Level II) Project Report entitled **Brain Tumor Segmentation and Area Calculation using Convolutional Neural Networks**, in partial fulfillment of the requirements for the award of the **Bachelor of Science** and submitted to the Department of Physics of University of Ruhuna is an authentic record of my own work carried out during a period from **January 2021 to April 2021** under the supervision of **Mr. Sameera Lakshan** Designation of supervisor(s), Physics Department.

The matter presented in this Project Report has not been submitted by me for the award of any other degree elsewhere.

Signature of Student

E.S.K.Chandrasekara

This is to certify that the above statement made by the student is correct to the best of my knowledge.

Signature of Supervisor

Date: **Mr. Sameera Lakshan**

Head

Department of Physics

Acknowledgements

I would like to place on record my deep sense of gratitude to Prof. G.D.K.Mahanama, HOD-Dept. of Physics, University of Ruhuna, Matara, Sri Lanka for his generous guidance, help and useful suggestions.

I express my sincere gratitude to Dr. N.M. Wickramage Dept. of Physics, University of Ruhuna, Matara, Sri Lanka, for her stimulating guidance, continuous encouragement and supervision throughout the course of present work.

I also wish to extend my thanks to Dr. K.V.S. Prasadh for his insightful comments and constructive suggestions to improve the quality of this project work.

I am extremely thankful to Mr. Sameera Lakshan for providing me infrastructural facilities to work in, without which this work would not have been possible.

Abstract

Physicians commonly employ Magnetic Resonance Imaging (MRI) scans to diagnose and plan treatments for brain tumours. Brain tumour segmentation is one of the most critical and complex challenges in medical image processing, as human-assisted manual categorization might result in incorrect prognosis and diagnosis. Furthermore, it is challenging work when there is a considerable volume of data to be processed. Because brain tumours have a wide range of characteristics and share many similarities with normal tissues, extracting tumour regions from images becomes difficult. It is considering that the medical profession is interested in automated segmentation algorithms due to the time-demanding nature of this task. This paper suggested extracting brain tumours from Magnetic Resonance Brain Images using Resunet architecture, followed by standard classifiers and a convolutional neural network. Although research investigates how deep learning may be used to split out tumours from MRI scans and calculate their area. The experiment was done using a dataset with a range of places, types, and image intensities. In the classifier section, we used traditional classifiers, namely the Resnet deep neural network, developed in Scikit-Learn. We then proceeded to Convolutional Neural Network (CNN) implementation using Keras and Tensorflow because it outperforms traditional ones. CNN achieved an accuracy of 72.64% and validation accuracy of 64.97% in our work, which is really impressive. Finally, the tumour is extracted from the MRI image, and the amount of area is calculated.

Table of Contents

List of Figures

List of Tables

Abbreviations

AI Artificial intelligence

UHC Universal Health Coverage

ML Machine Learning

CNN Convolutional Neural Networks

MRI Magnetic Resonance Imaging

CNS Central Nervous System

CSF Cerebrospinal Fluid

GBM Glioblastoma

EEG Electroencephalogram

CT Computed Axial Tomography

SPECT Single-photon Emission Computed Tomography

PET Positron Emission Tomography

fMRI Functional Magnetic Resonance Imaging

kNN k-Nearest Neighbours

SVM Support Vector Machines

RNN Recurrent Neural Networks

ANN Artificial Neural Networks

FCM Fuzzy C-Means

Chapter 1

Introduction

Artificial intelligence (AI) and related innovations are increasingly common in business and society and are starting to be applied to healthcare. These AI innovations can change many areas of health care, as well as work procedures within providers, payers, and pharmaceutical organisations. Although the medicine has been receptive to the advantages of big data and AI, it has been slow to adopt fast-moving technology, particularly in comparison to sectors such as finance, entertainment and transport, that is to say, to today.

The fundamental transformation of health systems is crucial to overcoming these obstacles and achieving Universal Health Coverage (UHC) by 2030. Machine Learning (ML), the most concrete representation of AI and the latest growth field of digital technology, possesses the capability of doing more and less and maybe a catalyst for such transformation [5]. However, the essence and scope of this pledge has not been systematically assessed.

At about the same time, the globe's population continues to grow longer and healthier than ever before and with the economic meltdown. Medical professionals are moving to value-based and encouraged care as non-communicable diseases such as diabetes, cancer and obesity are becoming global pandemics [39].

Healthcare professionals, individuals and organisations all provide a source of data that can be used for ML. Many people have a strong idea of what they would like to learn from the data but are unaware of how much data is needed and what can be done before

more technological aspects of uncovering hidden patterns, trends and assumptions are identified.

This report takes a realistic, practical approach to AI, ML, and Convolutional Neural Networks (CNN) and the ethical consequences of such methods. We cover some of the theoretical and practical applications of AI in brain segmentation with Magnetic Resonance Imaging (MRI) images from where and how to start applying CNN and evaluating results.

1.1 Problem Statement and Objectives

The purpose of this project is to build a model that examines the influence of a CNN on MRI segmented images. And also the tumour area on preoperative and postoperative MRI should be measured and compared to assess the resection extent. Finally, this combination produces improved outcomes and aids in disease detection in a more effective and timely manner.

1.2 Project Structure

This study proposes a novel method for segmenting MRI data that integrates components of the data to provide improved segmentation and area calculations. The MRI scanned images is used for the entire process in this project. For brain tumour segmentation and area calculation, various types of segmentation algorithms have been developed.

The first chapter outlines the motivation and introduces image segmentation as a method for quantitative research of MRI images. Chapter two reviews theoretical background approaches for entire process. Chapter three describes the study's literature review, which is based on different aspects of views relative to this study. Our approach is described in Chapter four, which includes baseline models and the segmentation pipeline. The five chapter examined the outcomes of each model. Chapter six provided conclusions and proposes topics for future work.

Chapter 2

Theoretical Background

This chapter will assist in comprehending the fundamental terms and concepts of the particular issue, which are needed to explain the problem and approach. This section describes the key scientific concepts, anatomical and physiological dimensions of the brain, MRI, and the major segmentation techniques to help you understand them.

2.1 The Brain

The brain is an amazing organ in humans and is a component of the Central Nervous System (CNS). It is encased by the skull and is made up of grey matter, white matter, and Cerebrospinal Fluid (CSF) [36]. The CSF delivers [12] nutrients and hormones to the brain. The grey matter is made up of neuron cell bodies, while the white matter is made up of myelinated axons.

The brain is divided into hundreds of anatomical areas, which we will explore in this section. Such as following the standard neuroanatomy hierarchies, diencephalon, including brainstem, cerebellum and cerebrum [52].

2.1.1 Brainstem

The brainstem, as seen in figure 2.1, is the posterior portion of the brain that attaches to the spinal cord. The midbrain, as well as the pons and medulla oblongata of the hindbrain, form the brainstem of the human brain. Considering task itself the main

motor and sensory nerve supply to the face and neck is provided by the brainstem through the cranial nerves [31].

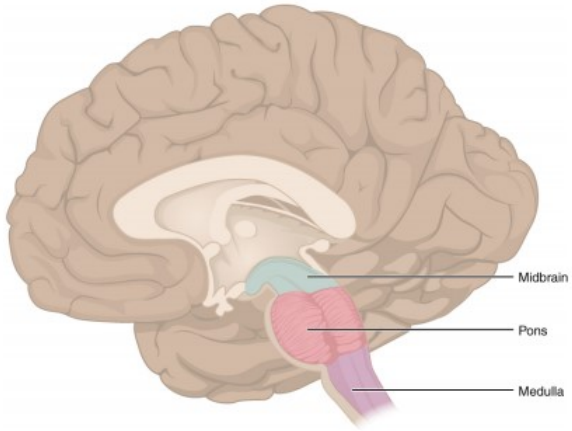

Figure 2.1: A figure of the brainstem [26]

2.1.2 Cerebrum

The cerebrum is the main component of the human brain, and it contains the cerebral cortex as well as other subcortical structures such as the hippocampus, basal ganglia, and olfactory bulb [33]. The cerebrum seems to be the uppermost area of the central nervous system in the human brain and which performs functions like movement, sensory processing, communication, or memory [34]. It is divided into four lobes, each with a distinct feature. Figure 2.2 depicts the brain and its lobes.

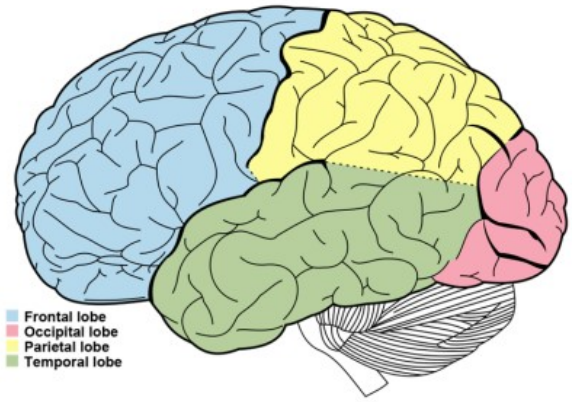

Figure 2.2: An illustration of human brain lobes [26]

2.1.3 Glioblastoma

Glioblastoma (GBM) seems to be the most common and lethal brain tumour, with exponential rise and bleak prognoses. It is a form of glioma that grows diffusely and infiltrating with no clear boundaries. The word "multiforme" is often used to characterise glioblastoma, suggesting that the tumour's pathologic presence is highly variable [24].

The tumour is most commonly located in the cerebral hemispheres' subcortical white matter. Patients with GBM are treated with surgical tumour resection, followed by radiotherapy and probably chemotherapy [22]. The extent of surgical removal has a significant impact on the patient's survival period. A resection that reduces 98% or more of the tumour volume results in a median survival period of 13 months, while a resection that removes less than 98% results in a median life expectancy of 8.8 months [22],[10]. The appropriate extent is determined by the tumor's size and quality, the patient's status and neurological condition, and the surgeon's practice.

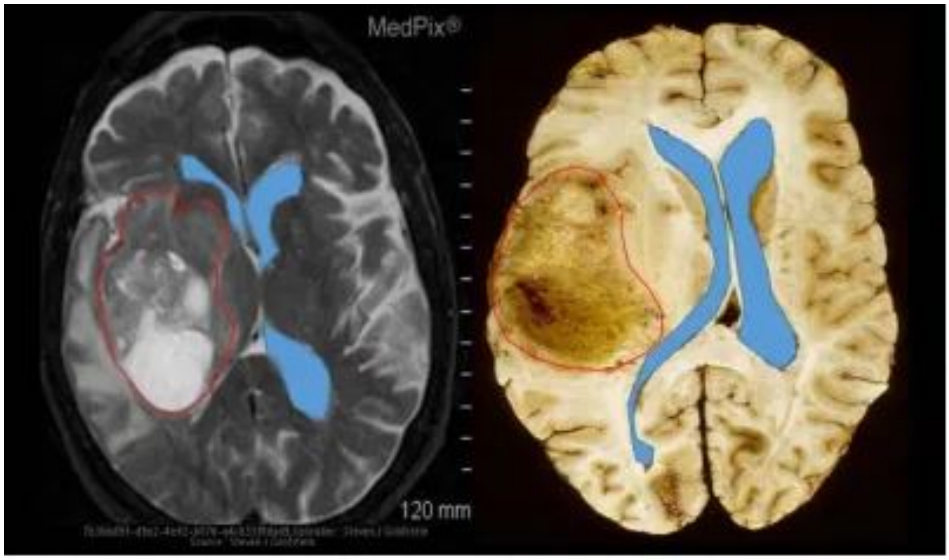

Figure 2.3: Two different glioblastomas from MedPix images

2.2 Introduction of the Tumour

A tumour is an abnormal mass that may occur within or on the brain. This anomalous and dysfunctional portion of the brain is referred to by two different names.

- Tumour
- Cancer

Tumors and cancer are not the same thing. A tumour is a mass of irregular tissues that can be solid or fluid-filled. As reference in [44] tumors are classified as either primary or secondary. Primary tumours are made up of cells from the organ in which the tumour is located. The nervous system primarily supports the growth of primary tumours, and tumour growth is very slow.

Cancer is the uncontrollable development of unhealthy tissues that harms the brain's nearby healthy tissues.

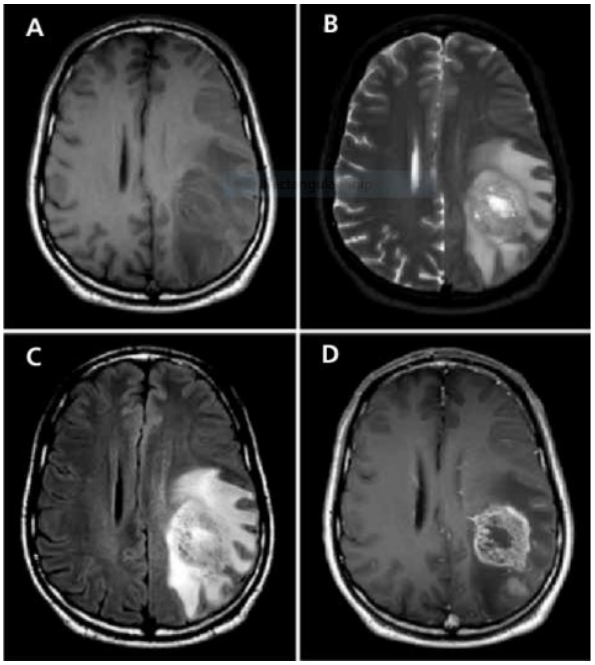

Figure 2.4: Brain tumor evaluation images which are taken from [42]

2.2.1 Brain Tumour

A brain tumour is an irregular development of tissue in the brain or the central spine that can interfere with normal brain function [40]. Healthcare professionals identify tumours based on where the tumour cells originated and whether they are cancerous (malignant) or not (benign). All brain tumours can develop and damage areas of normal brain tissue, which can be debilitating and potentially fatal.

As above mentioned tumours are classified as benign, malignant and pre-malignant [7],[18]. In this section, I intend to provide a general overview of both benign and malignant primary brain tumours in adults.

2.2.2 Benign Brain Tumor

A benign brain tumour is the least threatening form of brain tumour. They are formed by cells inside or surrounding the brain, do not include cancer cells, expand slowly, and have distinct boundaries that do not expand into the other tissue [35]. They could grow to be very broad before causing symptoms [7]. Although, depending on their size and position in the brain [18], they can cause severe neurological symptoms.

2.2.3 Malignant Brain Tumour

Malignant brain tumours include cancer cells which often lack distinct boundaries. They are labeled life-threatening due to their rapid growth and invasion of surrounding brain tissue [40]. Malignant brain tumours rarely travel to other parts of the human body, but they may spread across the brain or to the spine. These tumours may be cured with surgery [17], chemotherapy, and radiation, however they can occur frequently [11].

.

2.3 Principles and Methods of Neuroimaging

This section will go into several various approaches to neuroimaging techniques. Neuroimaging employs several methods to picture the Central Nervous System either directly or indirectly. The technique may either be Structural Imaging, which involves creating an image of the anatomy and pathology or injury, or Functional Imaging, which involves attempting to create a picture of the metabolic or pharmacologic reaction including its brain or cognitive functioning.[41]. There are several methods [25] available for obtaining structural or functional images of the nervous system.

- Electroencephalogram (EEG)
- Computed Axial Tomography (CT)
- Single-photon Emission Computed Tomography (SPECT)
- Positron Emission Tomography (PET)
- MRI
- Functional Magnetic Resonance Imaging (fMRI)

2.3.1 Basics of MRI

Magnetic Resonance Imaging, another nuclear imaging method, employs both static and variable magnetic fields to perturb hydrogen atoms. The disturbance of these hydrogen atoms results in a magnetic resonance, which is then calculated by radio-frequency coils. These radio-frequency receivers can translate these details into a three-dimensional image, and based on the tissue type, shorter wave sequences may be used to produce different contrasts. In the figure 2.7a and 2.7b below, you would see an MRI scanner and a schematic image of what it looks like inside. The variable magnetic fields can indeed be applied in various directions, and then the radio frequency coil can be used

to figure out the magnetic perturbance that you've been adding to the device, which can then be transformed into an image.

(a) MRI machine with a patient

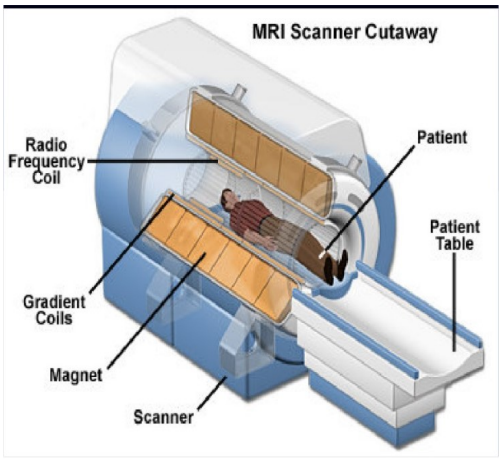

(b) Schematic image of MRI

Figure 2.5: (a) MRI machine with a patient and (b) Schematic image of MRI

2.3.2 Physics of MRI

In this section, we'll go into more depth on specifically the basics Physics of the MRI that is used to create MRI images. The majority of the human body 96% is composed of just four elements [47]. There are four of them: hydrogen, oxygen, carbon, and nitrogen. The most common element in the universe and in humans is hydrogen[47].

All we know atom is contained with Protons, Neutrons and Electrons. When examining the motion of an atom, there are three forms [47] of particle motion mostly in atom:

- Negatively charged electrons spinning on their own axis.
- Negatively charged electrons orbiting the nucleus.
- Particles within the nucleus spinning on their own axes.

Each form of motion above generates a magnetic field. We are interested in the motion of particles inside the nucleus as well as the nucleus itself in MRI. Inside the nucleus, protons and neutrons rotate on their own axis. Since the direction of spin is random, some particles rotate clockwise while others spin anticlockwise. When a nucleus has an

even mass number, the spins cancel each other out, resulting in no net spin but with an odd mass number that makes a spin [48].

A rotating unbalanced charge generates a magnetic field around itself due to the laws of electromagnetic induction 2.6a. A magnetic moment denotes the position and scale of the magnetic field. The magnitude of the magnetic moment is defined by the length of the arrow. And also the magnetic moment's alignment is indicated by the direction of the arrow 2.6b.

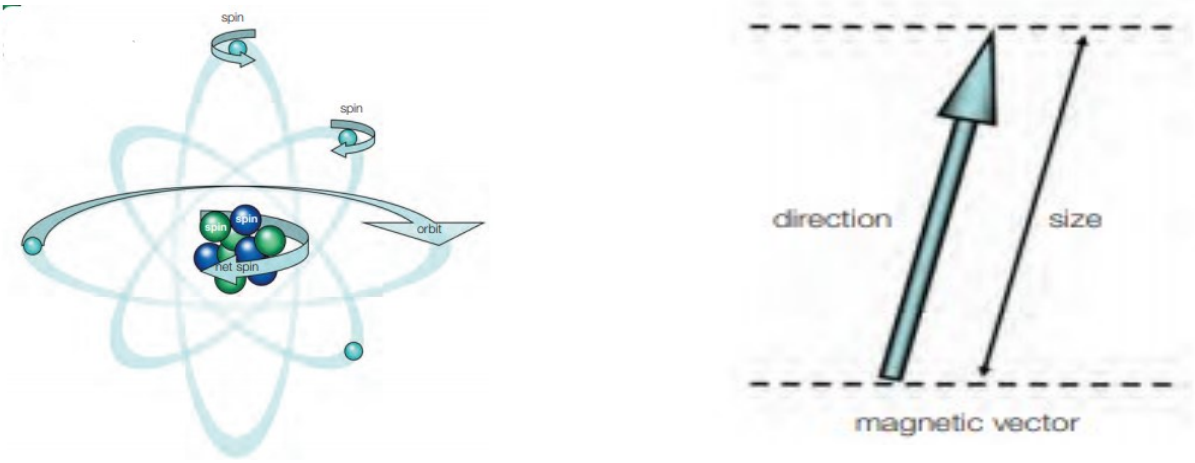

(a) The atom

(b) The magnetic moment of the H_2

Figure 2.6: Image (a) describes its atomic structure and behaviour (b) MG of hydrogen [47]

MR activity is described as nuclei with an odd number of protons. They work similarly to tiny bar magnets. Table 2.1 shows the spin characteristics of the most common MR active nuclei.

Element	**Protons**	**Neutrons**	**Nuclear spin**	**Natural abundance**
^{1}H(protium)	1	0	1/2	99.985
^{13}C(carbon)	6	7	1/2	1.10
^{15}N(nitrogen)	7	8	1/2	0.366
^{17}O(oxygen)	8	9	5/2	0.038

Table 2.1: Constants of selected MR active nuclei [47]

Protium, a hydrogen isotope, is used in MR imaging because [43, 47, 48]

- It is abundant in the human body (e.g. in fat and water).
- The solitary proton gives it a relatively large magnetic moment because there are no neutrons present in this type of nucleus 2.1.

,

Alignment

The magnetic moments of MR spins point in a random direction in a normal setting, producing no overall magnetic effect. As spins are positioned in an external magnetic field, their magnetic moments correspond with the flux lines of the magnetic field. This is known as alignment and it is describing using two theories as to the classical theory and the quantum theory.

Precession

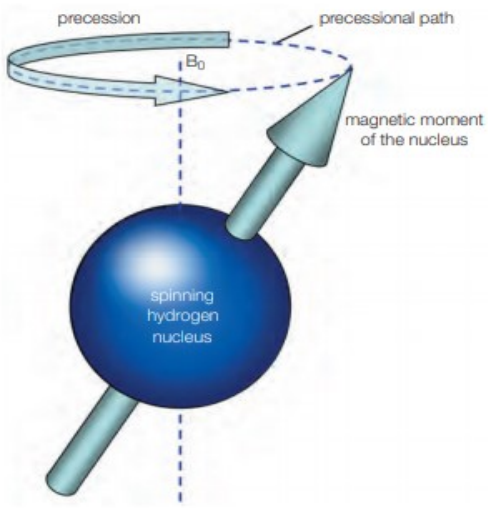

(a) Precession

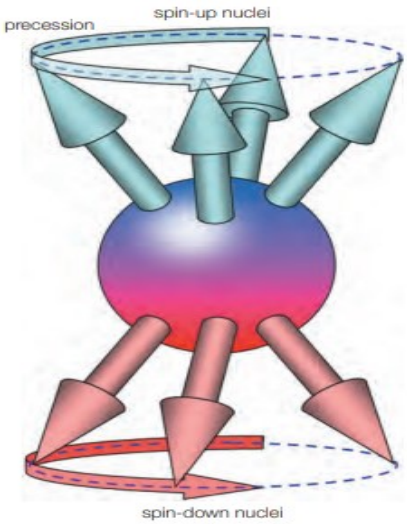

(b) Precession of the spin-up and spin-down populations

Figure 2.7: (a) Precessio and (b) Precession of the spin-up and spin-down populations [47]

As early discussed each MR active nucleus spins on its axis. The magnetic field induces a secondary spin by exerting a torque on the magnetic moments of all MR active nuclei. This spin is known as precession [6], and it induces all spin up and spin down to define a circular path around B_0 as in figure 2.7a. Although, the precessional frequency is the rate at which magnetic moments spin around the external magnetic field [32].

2.4 Machine Learning and Convolutional Neural Networks

Machine learning is concerned with developing algorithms that respond to the presentation of new data and the discovery of further information. Machine learning demonstrates data mining concepts, but it can also identify patterns, learn from them, and apply them to new algorithms. The aim is to imitate a human's ability to learn from experience when completing the given tasks without, or with limited, human assistance.

Whether it is supervised or unsupervised, the purpose of machine learning is a generalisation, or indeed the ability to perform well based on previous experiences [20]. There are two practical approaches to supervised machine learning: regression-based systems and classification-based systems [29]. Classification algorithms include decision trees, Nave Bayesian, logistic regression, k-Nearest Neighbours (kNN)), Support Vector Machines (SVM). Linear regression, regression trees, Support Vector Machines, k Nearest Neighbour, and perceptrons are examples of regression algorithms [29].

2.4.1 Artificial Neural Networks

And with their ability to model multidimensional data and identify hidden patterns in data, neural networks are well-suited for data mining tasks. Prediction and classification problems can be solved using neural networks [23]. Forward propagation refers to the method of estimating the outcome and comparing it to the actual output [38]. And also fully connected neural networks, convolutional neural networks, Recurrent Neural Networks (RNN), long short-term memory neural networks, autoencoders, deep

belief networks, generative adversarial networks trained with an algorithm called back-propagation [16].

Perceptrons are used to build Artificial Neural Networks (ANN), which have one or more hidden layers, as seen in below neural network chart. Backpropagation is the process of evaluating and propagating the error, or loss, at the output to the network. Weights are adjusted at each node to minimise the error performance from each neuron.

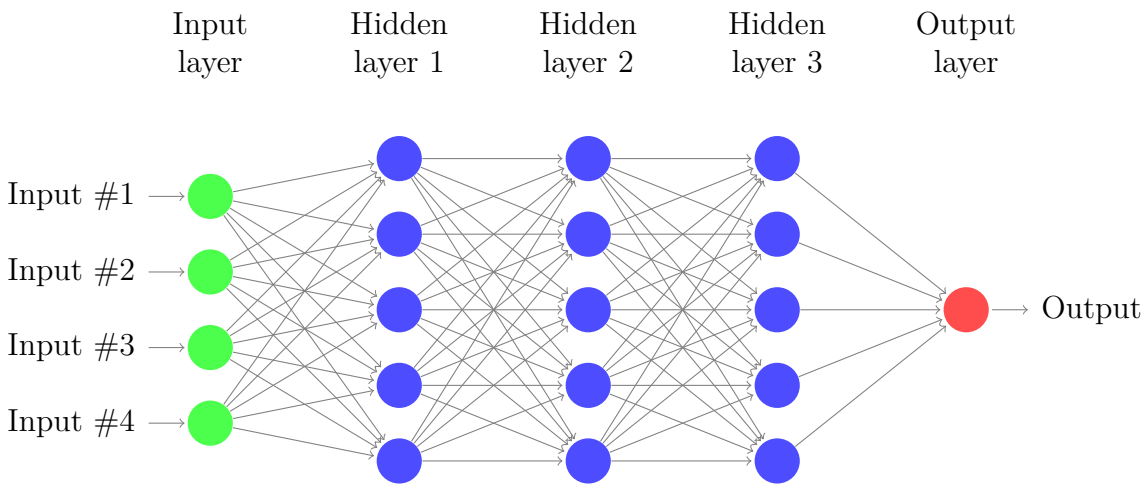

Figure 2.8: Architecture of neural networks

2.4.2 Convolutional Neural Network and Segmentation

Convolutional Neural Networks are made up of neurons that have different weights and biases [30]. The anterior layer provides some feedback to these neurons. It computes the dot product of the input and weights and, if desired, follows it with a non-linearity. Convolution layer contains several convolution layers with ReLU activation function and pooling phase [28]. In the end, the final layer is connected layer is a default neural network architecture as shown in the figure 2.8. Figure 2.9 Architecture of CNN.

Convolution Layers

The convolution layer aims to take or extract a component from the input images, and only the image part is linked to the next convolution layer. The dot product between

the receptive field and a kernel [3*3] on the entire image in CNN. The result of all of this is a single integer, which we can refer to as a feature map. We must repeat this process from the entire input image and measure the dot product with weights and biases to obtain the featured maps; the output of these layers is the input for the successive layers.

Padding Layers and Pooling Layers

Padding contains a zero layer beyond the input volume to ensure that information on the borders is not lost and we can get the same output dimension as the input volume.

The pooling layer reduces the dimension of the input image and controls overfitting. This study used max pooling, which takes the maximum value from the input image that we fully connected with the filter [3].

Activation Functions

After applying convolution to that same input volume, we must apply ReLU to the feature map to give the device non-linearity. We chose ReLU because it does not experience the vanishing gradient problem, which occurs when the first layer of a neural network runs slowly, causing it to fail to predict the correct performance and produce errors [1]. At the end of the neural network, we have to use the sigmoid function as an activation function. It is used for binary classification and is used in logistic regression for defining two classes [46].

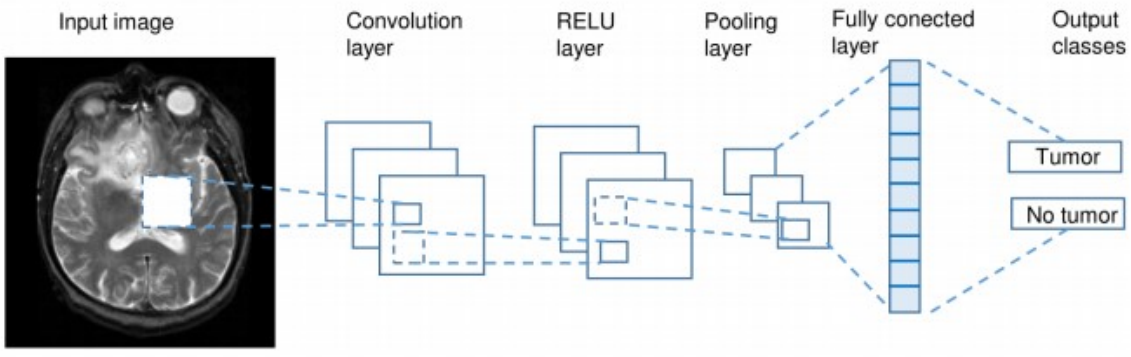

Figure 2.9: Architecture of CNN [21]

Chapter 3

Literature Review

Recently, Machine Learning and Deep Learning methods have been widely used for the identification and grading of brain tumors using various imaging methods, especially those obtained using CNN. Bower, J.M and Beeman, D propose [8] a system that combines with CNN for brain tumor classification. The proposed model attained an overall classification accuracy of 95.82%. Hasan [15] proposed a system for MRI brain scan classification using deep and handcrafted image features. Here Automatic feature extraction was done by CNN and Support Vector Machine (SVM) classification with a 10 fold cross-validations have shown 99.30 % accuracy on 600 axial MRI scans. The Naive Bayes-based brain tumor detection method [51] uses maximum entropy segmentation based on the threshold. The proposed approach has the advantage of being able to locate a tumor in all possible areas in the brain, including the temporal lobe. Seetha. J and S.S. Raja [2] suggested a deep CNN method for automatic brain tumor identification and grading. The system is based on Fuzzy C-Means (FCM) for brain segmentation and The results showed that the method achieved a rate of 97.5 percent accuracy.

Chapter 4

Materials & Methods

As the title suggests, this chapter contains the study's project methodology. This section begins by focusing on the patient data sets used as well as the development environment. Furthermore, the methods for segmentation, visualisation, and area measurement and the evaluation techniques used are described in detail.

4.1 Research Strategy

In the section 4.3 data set has given 3929 MRI scans along with their brain tumour location (figure 4.1). The flowchart provided will show the strategy and actions taken to achieve the study's goal and approach its conclusion stage.

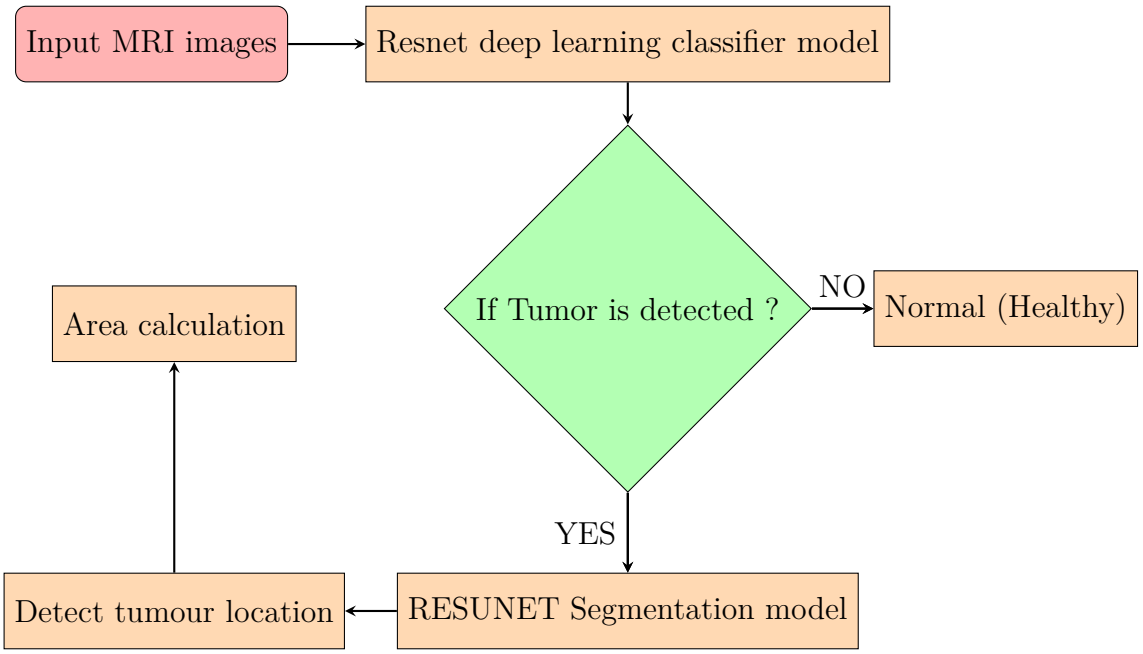

4.2 Softwares

The programming is done in MATLAB and Python. MATLAB version is (R2015a, 64-bit) from MathWorks, Inc. (Natick, MA; United States). In python, the Google Colab platform was used with High-performance GPU access to complete the whole task.

4.3 Datasets

For the algorithm development, training and testing data were used. It contained 111 image folders that have tumour images and its mask images. It also has two CSV files that will help identify the patients' details and whether it has a tumour or not. Two CSV files shows data.csv and its datamask.csv.

Data collected from previous researchers' brain tumour classification techniques, on which comparisons will be made based on various attributes such as, technique and accuracy. Various types of MRI Images will be available depending on the need. Figure 4.1 shows details all about the patients' tumour image and its mask image. Those all the tumour images have saved in .tif file format.

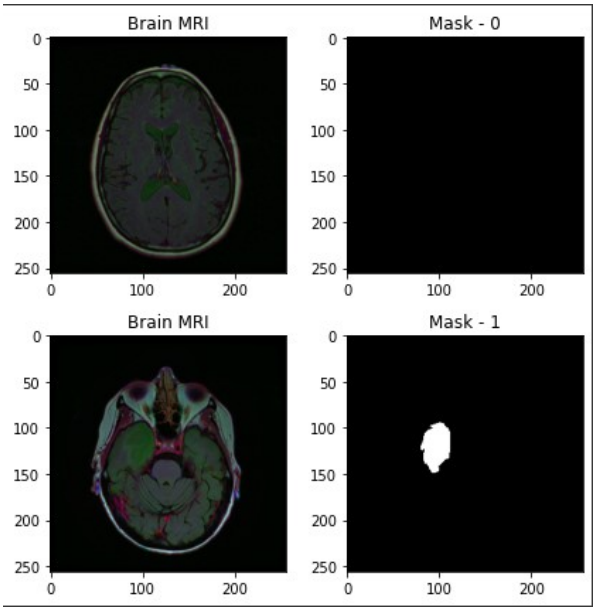

Figure 4.1: Brain tumour display by using python.

Although you can see figure 4.2 shows patients details. Table 4.1 describes all the numerical information as well. As shown in table 4.1, we can see there are 2556 amount of patient healthy and 1373 patients detected they have a tumour.

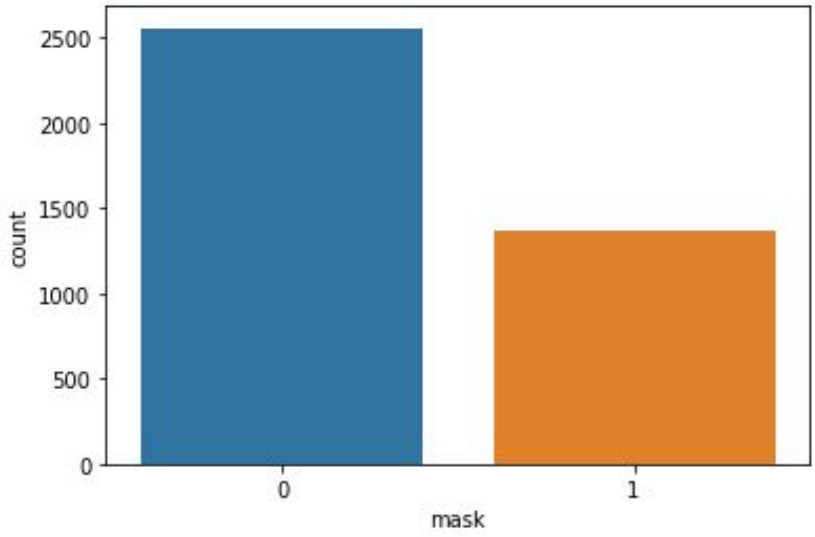

Figure 4.2: Patient details with count plot.

Results	Tumour or not	Amount
0	Tumour not	2556
1	Tumour	1373

Table 4.1: Patients details

4.4 Data Analysis Technique and Segmentation

The collected data will be evaluated and compared based on various attributes. Therefore a technique or algorithm is used to examine brain MRI images. The obtained data will be evaluated and compared based on particular features. A technique or algorithm that is used to examine brain MRI images. Convolutional Neural Network [28] will be used to classify MRI images in the proposed model. Although, ResNet [9] architecture will be used during the given task. And also, when we are concerned about segmentation, picture segmentation is a technique that divides images into sections based on similarities, with each part (pixel) containing similar features [49].

4.4.1 Image Segmentation

Image segmentation seeks to comprehend and extract information from images at the pixel level [14]. Image segmentation can also be used for object detection and localization, which has a wide range of applications including medical imaging and self-driving vehicles [4]. Nowadays, we can see Modern image segmentation techniques are based on a deep learning approach that employs common architectures like CNN, FCNN, and Deep Encoders-Decoders [50]. However, in case of Unet, we convert (encode) the image into a vector followed by up sampling (decode) it back again into an image. For each pixel in the input image, U-net calculates a loss function. The Softmax function is applied to each pixel, transforming the segmentation problem into a classification. And also you can see figure 4.3 shows process of the ResUnet.

Figure 4.3: Brain tumour segmentation by using ResUNet architecture.

4.4.2 Deep Residual Learning and ResNet architecture

Deeper neural networks need more effort to train, not because of the computational expense because of the difficulty in propagating gradients across many layers. Neural networks learn by computing variable derivatives concerning the training loss function. However, with too many deep layers, derivatives begin to diminish, a phenomenon known as gradient vanishing [50]. The authors introduced residual connections into the network to solve the gradient vanishing problem associated with ultra-deep networks. Residual connections are essentially connections between one layer and the layer above it.

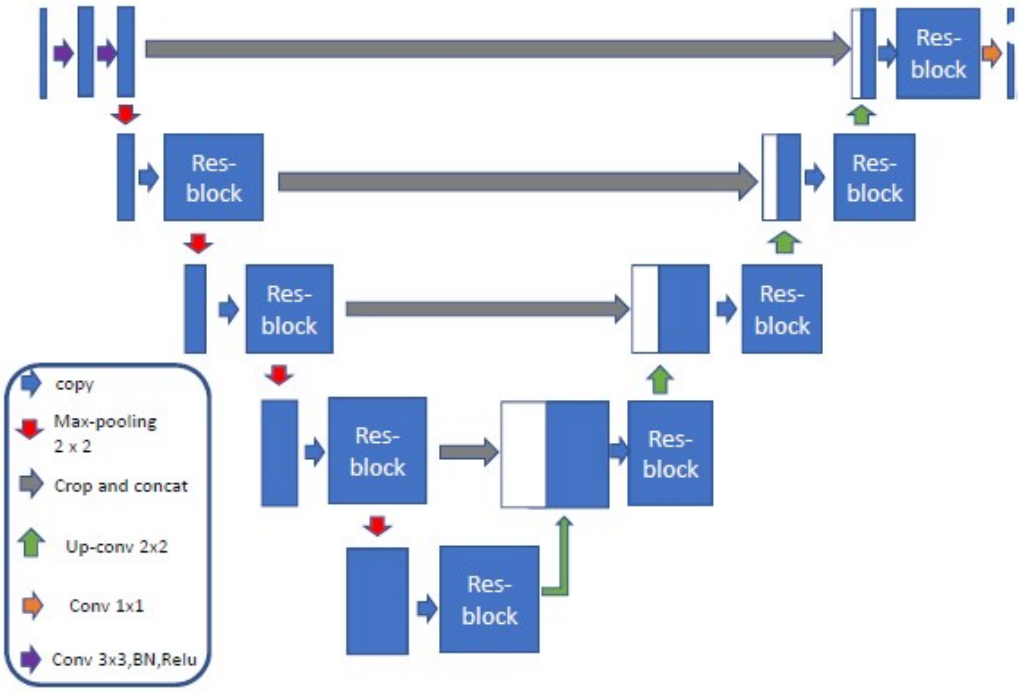

Figure 4.4: ResUNet architecture.

ResUNet architecture combines UNet backbone architecture with residual blocks to overcome the vanishing gradients problems present in deep architectures. Unet architecture is focused entirely on convolutional networks and has been modified to perform well on segmentation tasks. Resunet consists of three parts. They are encoder or contracting path, bottleneck and decoder or expansive path.

When consider the ResUNet architecture (figure 4.4), encoder or contracting path consist of 4 blocks (left sides first blocks). First block consists of 3×3 convolution layer + Relu + Batch-Normalization. Remaining three blocks consist of Res-blocks followed by Max-pooling 2×2. Although bottleneck is in-between the contracting and expanding path. Which consist of Res-block followed by up sampling conv layer 2×2. Expanding or decoder path consist of 4 blocks as well as (right side first four blocks). 3 blocks following bottleneck consist of Res-blocks followed by up-sampling convolution layer 2×2. Here you can see also, final block consist of Res-block followed by 1×1 convolution layer.

Chapter 5

Results & Discussion

This section describes the results and discussion obtained during the project. In the given data sets have the original MRI image and its mask as well. In section 4.3 we have already discussed data sets in detail. Although, for all test users, the segmentation properties (CNN, ResUNet) were chosen as proposed in section 4.4.

5.1 Results

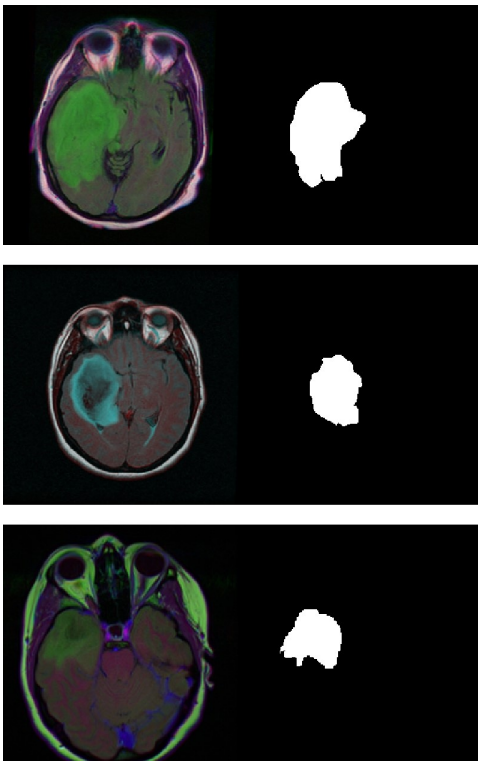

Figure 5.1: MRI image and its contour image.

The MRI enhanced sequences of the data sets were used to perform segmentation, visualisation, and area estimation on pre-operative images. Given data set 4.3 sets were segmented by above mentioned (4.4.1,4.4.2) algorithms to obtain evaluation data. The initial contour relative to its original MRI image was shown as given in figure 5.1. And also, you can see the figure 5.2 illustrates MRI tumour identification and which coloured with a red mask.

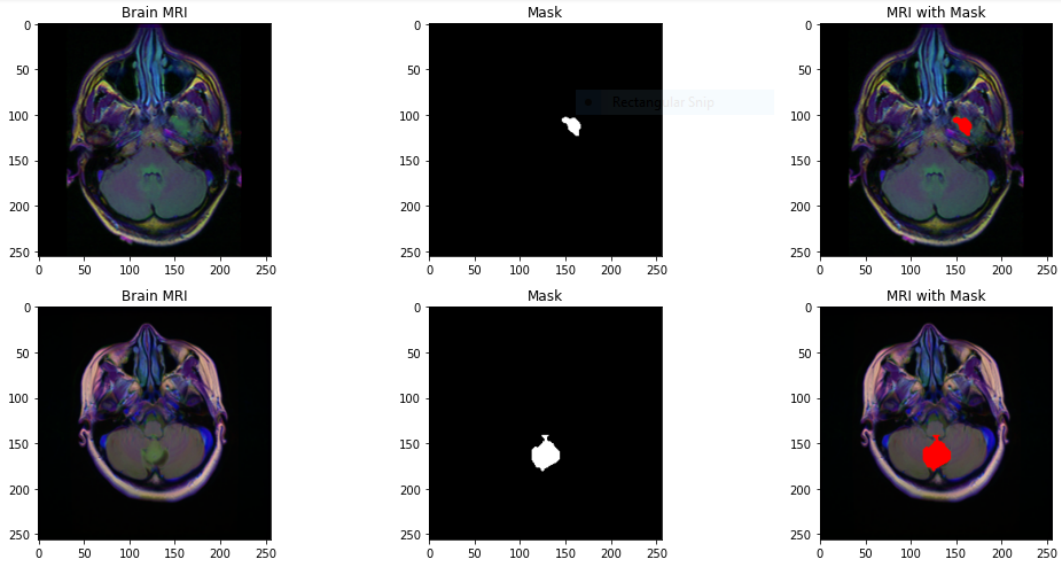

Figure 5.2: Tumour identification and colored in red mask.

5.1.1 Confusion Matrix

In general, Confusion Matrix [45] is a tool that aids in determining whether or not the model is performing satisfactorily. Furthermore, numerous evaluation measures, including accuracy, precision, recall, and so on, can be derived from it [13]. It is predicated on the concept that we may compare the class predicted by the classifier to the actual class for each observation. So, using this confusion matrix, we can see how efficient a model is. Each column represents the predicted class, while each row represents the actual class. Predictions from a binary classifier with values 0 and 1 are categorised into true positives, false negatives, false positives, and true negatives. Considering above mentioned task, you can see below the confusion matrix figures represent each epoch.

As previously stated, the efficiency of a model may be determined utilising this confusion matrix. Each column represents the predicted class, as each row represents the actual class. Furthermore, prediction results can see figure 5.4, which indicates the model's prediction accuracy and validation accuracy are 0.7284 and 0.6497 in respectively.

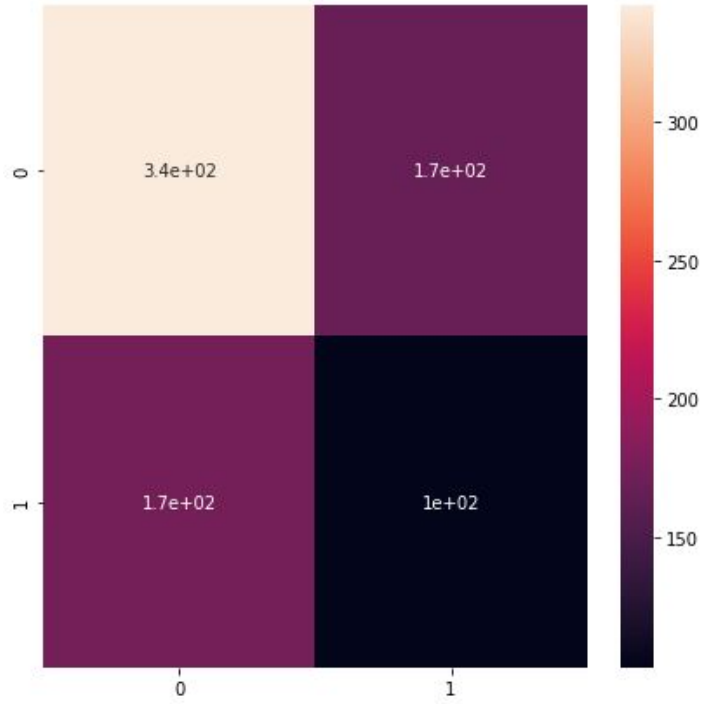

Figure 5.3: Heat map of confusion matrix

For the following task, we obtained a confusion matrix for epoch 1, as shown in figure 5.3. To explain in simple words the concepts beyond the confusion matrix table 5.1 will help you to understand.

		Predicted Classes		
		Positive	Negative	Total
Actual Classes	Positive	TN	FP	$TN + FP$
	Negative	FN	TP	$FN + TP$
	Total	$TN + FN$	$FP + TP$	N

Table 5.1: Confusion matrix

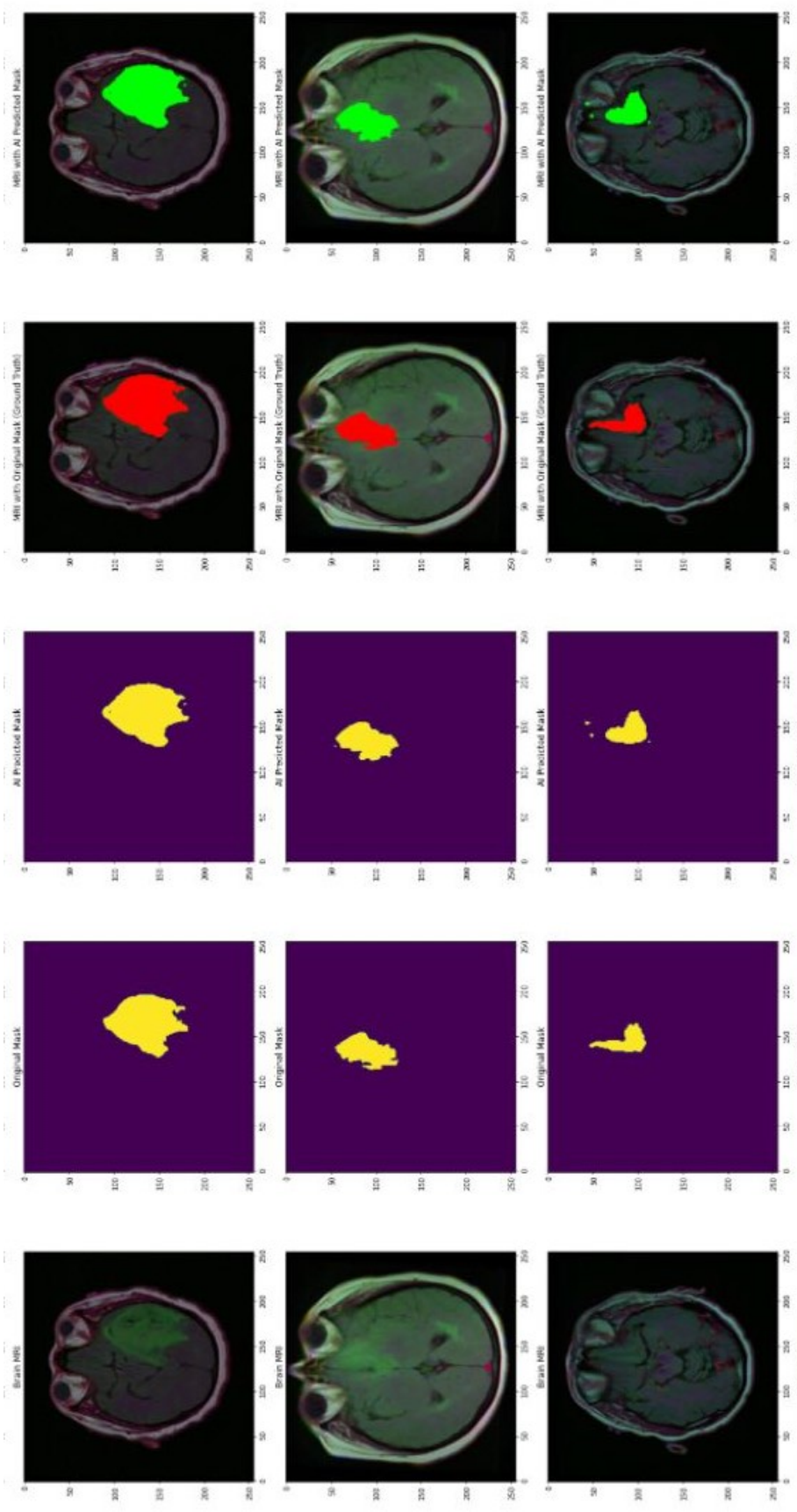

Figure 5.4: Predicted output

5.1.2 Area Calculation

In this chapter, we were able to get results of area calculation and correspond to its MRI, preprocess the image for contour extraction, recognize the reference object from the image and estimate its surface area and surface area evaluation of the target.

A contour is essentially a closed curve that connects all contiguous pixels that have a colour or intensity. A contour is a form found in an image that represents the shape of an object. As shown given, figures 5.5a and 5.5b represent the original MRI image, and it does not allow to get proper extraction of the tumour. Therefore all you can realise we have to extract a contour image before the calculation of the area.

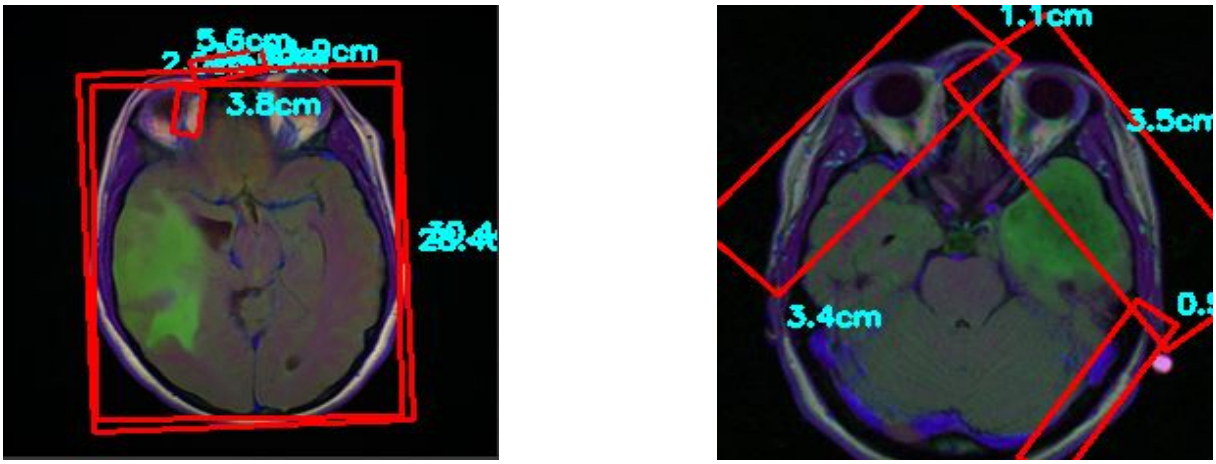

(a) (b)

Figure 5.5: MRI image with boundary box

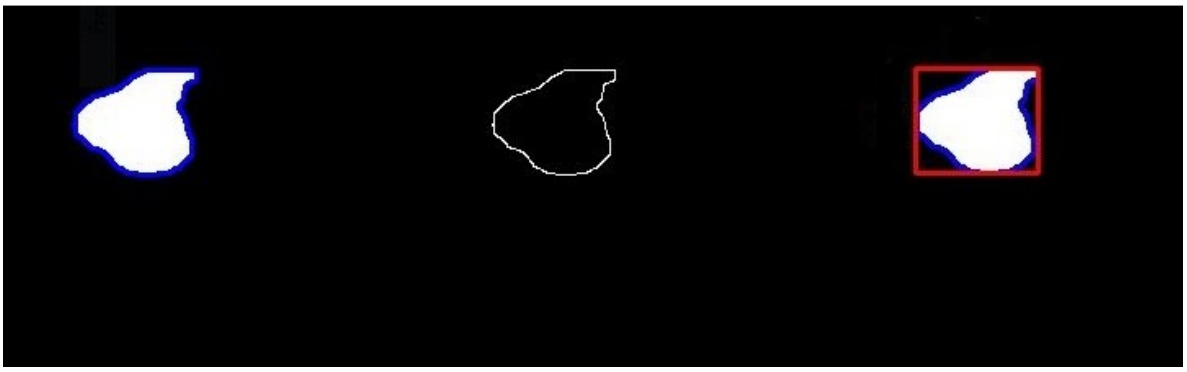

Figure 5.6: Tumour extraction and contour image.

Figure 5.6 is about tumour extraction of figure 5.5b and finally able to get result of contour image.

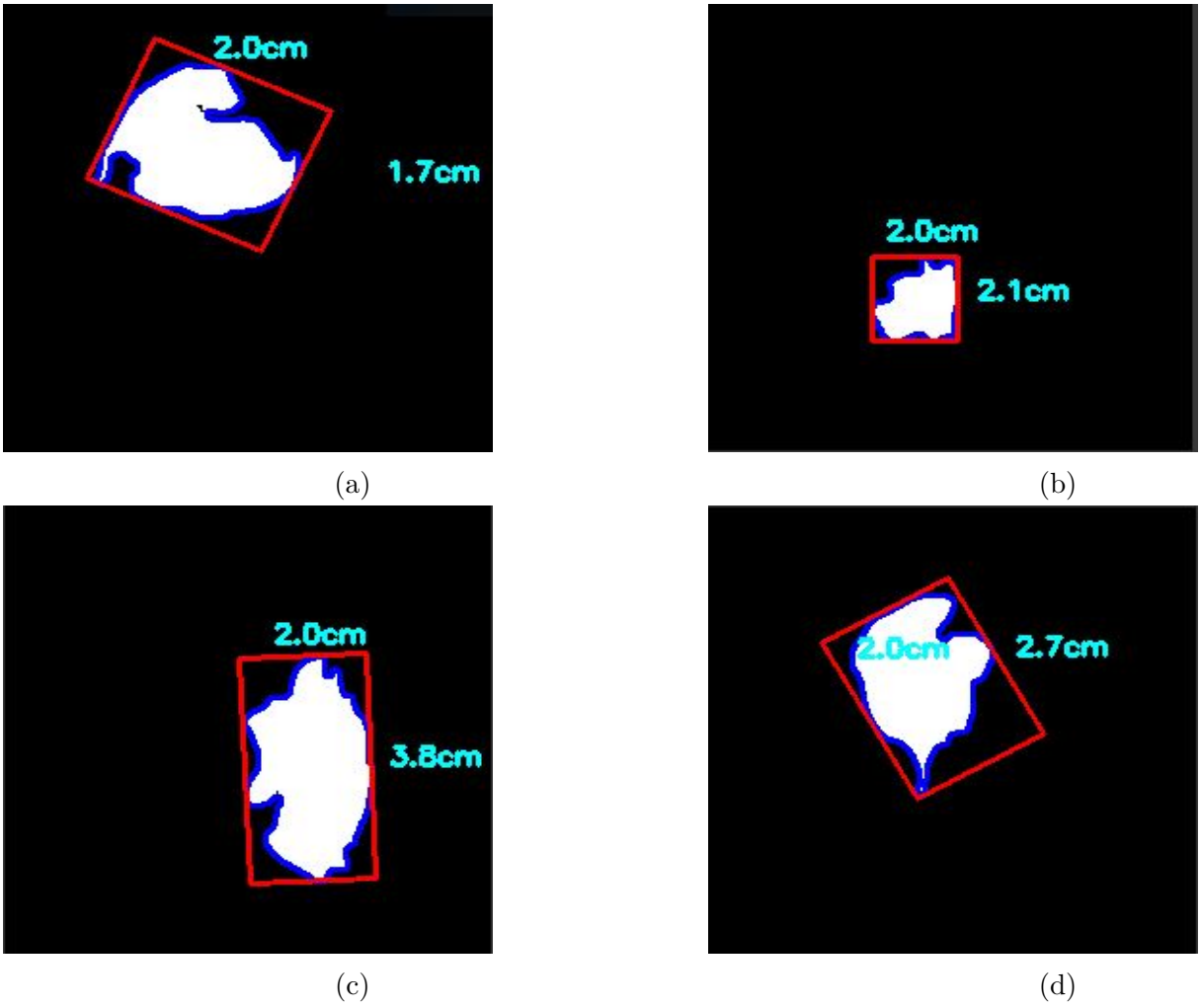

(a) (b)

(c) (d)

Figure 5.7: Area calculation of contour images

Area (Pixels)	Perimeter (Pixels)
5434.0	367.46
1433.5	184.95
5520.5	393.61
4382.5	349.81

Table 5.2: Area and Perimeter

The above, as shown in the figure 5.7, illustrate the area of the contour with parameters pixel. And also given table 5.2 below represents the numerical values of the area and perimeter. Randomly above four figures (5.7a, 5.7b, 5.7c and 5.7d) have chosen.

5.2 Discussion

In this project, We were tasked with increasing the speed and accuracy of detecting and localising brain tumours using MRI scans. To processing, We are given 3929 brain MRI scans as well as the locations of their brain tumours. You can see in the section 5.1 we illustrated both the brain image and its mask.

In this task, we trained the classifier model to detect whether a tumour existed or not. We trained two deep neural networks; the first one is Resnet deep learning classifier model, which explains if there's a tumour that has been detected or not. When the tumour has been detected, we trained another network, that ResUnet segmentation model, to localise the tumour in the actual image. To split the data to test and train, we have used testing size in 20%, which means that 80% will be allocated for training. To make sure this model can generalise, not memorise, we used a cross-validation data set as in 15%.

After downloaded the pre-trained Resnet50 model, we can see the summary of the model from compiled python code. Adding the classification head to the base model will be connected dense, fully connected artificial neural networks. In this model, each dense layer has 256 neurons, and the activation function is Relu [1]. And also, 30% drop out used for improve the generalising the capability of model.

We tested various optimizers and learning rates and discovered that the Adam optimizer [53] with a learning rate of 0.05 offered the most steady training. We trained for a total of 1,10,20 and 50 epochs in respectively on Google Colab GPU [37]. We opted to stop at the early mentioned levels because the training loss appeared to be decreasing, and it wasn't easy to operate without a strong GPU. After this process, we were able to obtain the result of the segmentation and finally the predicted results of the model.

For measuring the area of the contour image tumour, OpenCV [19] played a significant role in this process. Before calculating the area, we must ensure that the boundary lines are bound to the desired tumour region.

Chapter 6

Conclusions & Future Works

In this project, we investigated the application of deep learning to medical imaging. An experiment was carried out to detect the tumour from MRI scans and its area calculation. We employed the ResUnet architecture to segment brain tumours from MRI scans and evaluated several iterations to get an accurate result. Our approaches were reasonably accurate in segmenting the enhancing tumour, and although it did not perform well on several outliers in the validation dataset due to poor computer performance. The segmentation was carried by utilising an MRI image database that contains two types of MRI images, the original MRI and its mask. Our designed deep neural network is on pre-trained ResUnet architecture, and it is possible to get accurate results in several epochs. We trained four kinds of different epochs as 1, 10, 20, and 50 and finally able to get a good accuracy of the model.

In the future, the implemented segmentation method can be extended in a variety of ways. The far more crucial thing to do is to correct the under fittings and overfitting of the model. Although, One of the most significant advancements will be modifying the architecture such that it may be used during surgery for identifying and correctly finding tumours [27].

References

[1] Abien Fred Agarap. 'Deep learning using rectified linear units (relu)'. In: *arXiv preprint arXiv:1803.08375* (2018).

[2] Ali Mohammad Alqudah et al. 'Brain Tumor Classification Using Deep Learning Technique–A Comparison between Cropped, Uncropped, and Segmented Lesion Images with Different Sizes'. In: *arXiv preprint arXiv:2001.08844* (2020).

[3] SP Archa and C Sathish Kumar. 'Segmentation of Brain Tumor in MRI images using CNN with Edge Detection'. In: *2018 International Conference on Emerging Trends and Innovations in Engineering and Technological Research (ICETIETR)*. IEEE. 2018, pp. 1–4.

[4] Xabier Artaechevarria, Arrate Munoz-Barrutia and Carlos Ortiz-de-Solórzano. 'Combination strategies in multi-atlas image segmentation: application to brain MR data'. In: *IEEE transactions on medical imaging* 28.8 (2009), pp. 1266–1277.

[5] Omar Badawi et al. 'Making big data useful for health care: a summary of the inaugural mit critical data conference'. In: *JMIR medical informatics* 2.2 (2014), e22.

[6] Oliver Bieri and Klaus Scheffler. 'Fundamentals of balanced steady state free precession MRI'. In: *Journal of Magnetic Resonance Imaging* 38.1 (2013), pp. 2–11.

[7] Peter McL Black. 'Brain tumors'. In: *New England Journal of Medicine* 324.22 (1991), pp. 1555–1564.

[8] S Deepak and PM Ameer. 'Automated Categorization of Brain Tumor from MRI Using CNN features and SVM'. In: *Journal of Ambient Intelligence and Humanized Computing* (2020), pp. 1–13.

[9] Foivos I Diakogiannis et al. 'Resunet-a: a deep learning framework for semantic segmentation of remotely sensed data'. In: *ISPRS Journal of Photogrammetry and Remote Sensing* 162 (2020), pp. 94–114.

[10] 'Extent of resection and survival in glioblastoma multiforme: identification of and adjustment for bias'. In: *Neurosurgery* 62.3 (2008), pp. 564–576.

[11] Anna R Giovagnoli. 'Quality of life in patients with stable disease after surgery, radiotherapy, and chemotherapy for malignant brain tumour'. In: *Journal of Neurology, Neurosurgery & Psychiatry* 67.3 (1999), pp. 358–363.

[12] Jeremy R Gray, Christopher F Chabris and Todd S Braver. 'Neural mechanisms of general fluid intelligence'. In: *Nature neuroscience* 6.3 (2003), pp. 316–322.

[13] Sepand Haghighi et al. 'PyCM: Multiclass confusion matrix library in Python'. In: *Journal of Open Source Software* 3.25 (2018), p. 729.

[14] Robert M Haralick and Linda G Shapiro. 'Image segmentation techniques'. In: *Computer vision, graphics, and image processing* 29.1 (1985), pp. 100–132.

[15] Ali M Hasan et al. 'Combining deep and handcrafted image features for MRI brain scan classification'. In: *IEEE Access* 7 (2019), pp. 79959–79967.

[16] Robert Hecht-Nielsen. 'Theory of the backpropagation neural network'. In: *Neural networks for perception*. Elsevier, 1992, pp. 65–93.

[17] Jan J Heimans and Martin JB Taphoorn. 'Impact of brain tumour treatment on quality of life'. In: *Journal of neurology* 249.8 (2002), pp. 955–960.

[18] Jay Jagannathan et al. 'Benign brain tumors: sellar/parasellar tumors'. In: *Neurologic clinics* 25.4 (2007), pp. 1231–1249.

[19] Fares Jalled and Ilia Voronkov. 'Object detection using image processing'. In: *arXiv preprint arXiv:1611.07791* (2016).

[20] Michael I Jordan and Tom M Mitchell. 'Machine learning: Trends, perspectives, and prospects'. In: *Science* 349.6245 (2015), pp. 255–260.

[21] Justin Ker et al. 'Deep learning applications in medical image analysis'. In: *Ieee Access* 6 (2017), pp. 9375–9389.

[22] Michel Lacroix et al. 'A multivariate analysis of 416 patients with glioblastoma multiforme: prognosis, extent of resection, and survival'. In: *Journal of neurosurgery* 95.2 (2001), pp. 190–198.

[23] Pat Langley. *Elements of machine learning*. Morgan Kaufmann, 1996.

[24] David N Louis et al. 'The 2007 WHO classification of tumours of the central nervous system'. In: *Acta neuropathologica* 114.2 (2007), pp. 97–109.

[25] Antoine Louveau et al. 'Structural and functional features of central nervous system lymphatic vessels'. In: *Nature* 523.7560 (2015), pp. 337–341.

[26] Frederic Martini et al. *Anatomy and Physiology'2007 Ed*. Rex Bookstore, Inc., 2006.

[27] Sara Moccia et al. 'Toward improving safety in neurosurgery with an active handheld instrument'. In: *Annals of biomedical engineering* 46.10 (2018), pp. 1450–1464.

[28] Keiron O'Shea and Ryan Nash. 'An introduction to convolutional neural networks'. In: *arXiv preprint arXiv:1511.08458* (2015).

[29] Arjun Panesar. *Machine learning and AI for healthcare*. Springer, 2019.

[30] Krishna Pathak et al. 'Classification of brain tumor using convolutional neural network'. In: *2019 3rd International conference on Electronics, Communication and Aerospace Technology (ICECA)*. IEEE. 2019, pp. 128–132.

[31] George Paxinos and Xu-Feng Huang. *Atlas of the human brainstem*. Elsevier, 2013.

[32] Thomas William Redpath. 'Signal-to-noise ratio in MRI.' In: *The British Journal of Radiology* 71.847 (1998), pp. 704–707.

[33] Albert L Rhoton Jr. 'The cerebrum'. In: *Neurosurgery* 51.suppl_4 (2002), S1–1.

[34] Albert L Rhoton Jr. 'The cerebrum'. In: *Neurosurgery* 61.suppl_1 (2007), SHC–37.

[35] Elaine Ron et al. 'Tumors of the brain and nervous system after radiotherapy in childhood'. In: *New England Journal of Medicine* 319.16 (1988), pp. 1033–1039.

[36] Zack Y Shan et al. 'Neuroimaging characteristics of myalgic encephalomyelitis/chronic fatigue syndrome (ME/CFS): a systematic review'. In: *Journal of translational medicine* 18.1 (2020), pp. 1–11.

[37] Sarjil Shariar and KM Azharul Hasan. 'GPU Accelerated Indexing for High Order Tensors in Google Colab'. In: *2020 IEEE Region 10 Symposium (TENSYMP)*. IEEE. 2020, pp. 686–689.

[38] Qeethara Kadhim Al-Shayea. 'Artificial neural networks in medical diagnosis'. In: *International Journal of Computer Science Issues* 8.2 (2011), pp. 150–154.

[39] Orlando Simpson and Sergio G Camorlinga. 'A Framework to Study the Emergence of Non-Communicable Diseases'. In: *Procedia computer science* 114 (2017), pp. 116–125.

[40] Sheila K Singh et al. 'Identification of human brain tumour initiating cells'. In: *nature* 432.7015 (2004), pp. 396–401.

[41] Stephen M Smith et al. 'Advances in functional and structural MR image analysis and implementation as FSL'. In: *Neuroimage* 23 (2004), S208–S219.

[42] Shawn M Stevens et al. 'Idiopathic intracranial hypertension: contemporary review and implications for the otolaryngologist'. In: *The Laryngoscope* 128.1 (2018), pp. 248–256.

[43] Sanaz Taghizadeh and James Lincoln. 'MRI experiments for introductory physics'. In: *The Physics Teacher* 56.4 (2018), pp. 266–268.

[44] PM Thompson et al. 'Cortical variability and asymmetry in normal aging and Alzheimer's disease.' In: *Cerebral Cortex (New York, NY: 1991)* 8.6 (1998), pp. 492–509.

[45] James T Townsend. 'Theoretical analysis of an alphabetic confusion matrix'. In: *Perception & Psychophysics* 9.1 (1971), pp. 40–50.

[46] Anjar Wanto et al. 'Use of binary sigmoid function and linear identity in artificial neural networks for forecasting population density'. In: *IJISTECH (International Journal of Information System & Technology)* 1.1 (2017), pp. 43–54.

[47] Catherine Westbrook. *MRI at a Glance*. John Wiley & Sons, 2016.

[48] Catherine Westbrook and John Talbot. *MRI in Practice*. John Wiley & Sons, 2018.

[49] Roland Wilson and Michael Spann. *Image segmentation and uncertainty*. Research Studies Press Ltd., 1988.

[50] Minghao Yin et al. 'On the Mathematical Understanding of ResNet with Feynman Path Integral'. In: *arXiv preprint arXiv:1904.07568* (2019).

[51] Hein Tun Zaw, Noppadol Maneerat and Khin Yadanar Win. 'Brain tumor detection based on Naıve Bayes Classification'. In: *2019 5th International Conference on Engineering, Applied Sciences and Technology (ICEAST)*. IEEE. 2019, pp. 1–4.

[52] Jiawei Zhang. 'Secrets of the brain: an introduction to the brain anatomical structure and biological function'. In: *arXiv preprint arXiv:1906.03314* (2019).

[53] Zijun Zhang. 'Improved adam optimizer for deep neural networks'. In: *2018 IEEE/ACM 26th International Symposium on Quality of Service (IWQoS)*. IEEE. 2018, pp. 1–2.

Appendix A
Some Random Python Code

This template includes the library packages that I have used during the project. This template includes the library packages that I have used during the project. Some library help to run code instead of typing scratch of the code.

```
import pandas as pd
import numpy as np
import seaborn as sns
import matplotlib.pyplot as plt
import zipfile
import cv2
import os
import glob
import random
import ReduceLROnPlateau, EarlyStopping, ModelCheckpoint,
↪  LearningRateScheduler
from skimage import io
import tensorflow as tf
from tensorflow.python.keras import Sequential
from tensorflow.keras import layers, optimizers
from tensorflow.keras.applications import DenseNet121
from tensorflow.keras.applications.resnet50 import ResNet50
from tensorflow.keras.layers import *
from tensorflow.keras.models import Model, load_model
from tensorflow.keras.initializers import glorot_uniform
from tensorflow.keras.utils import plot_model
from tensorflow.keras.callbacks
from IPython.display import display
from tensorflow.keras import backend as K
from sklearn.preprocessing import StandardScaler, normalize
from google.colab import files
%matplotlib inline
```

In this project, we compiled, as shown below, python code to visualize the results of figure 5.4.

```
count = 0
fig, axs = plt.subplots(10, 5, figsize=(30, 50))
for i in range(len(df_pred)):
  if df_pred['has_mask'][i] == 1 and count < 10:
    # read the images and convert them to RGB format
    img = io.imread(df_pred.image_path[i])
    img = cv2.cvtColor(img, cv2.COLOR_BGR2RGB)
    axs[count][0].title.set_text("Brain MRI")
    axs[count][0].imshow(img)

    # Obtain the mask for the image
    mask = io.imread(df_pred.mask_path[i])
    axs[count][1].title.set_text("Original Mask")
    axs[count][1].imshow(mask)

    # Obtain the predicted mask for the image
    predicted_mask =
    ↪  np.asarray(df_pred.predicted_mask[i])[0].squeeze().round()
    axs[count][2].title.set_text("AI Predicted Mask")
    axs[count][2].imshow(predicted_mask)

    # Apply the mask to the image 'mask==255'
    img[mask == 255] = (255, 0, 0)
    axs[count][3].title.set_text("MRI with Original Mask (Ground
    ↪  Truth)")
    axs[count][3].imshow(img)

    img_ = io.imread(df_pred.image_path[i])
    img_ = cv2.cvtColor(img_, cv2.COLOR_BGR2RGB)
    img_[predicted_mask == 1] = (0, 255, 0)
    axs[count][4].title.set_text("MRI with AI Predicted Mask")
    axs[count][4].imshow(img_)
    count += 1

fig.tight_layout()
```